Synthesis, Structure, and Properties of the $[E_7M(CO)_3]^{3-}$ Complexes Where E = P, As, Sb and M = Cr, Mo, W

Scott Charles,† Bryan W. Eichhorn,*,† Arnold L. Rheingold,‡ and Simon G. Bott§

Contribution from the Department of Chemistry and Biochemistry, University of Maryland, College Park, Maryland 20742, Department of Chemistry, University of Delaware, Newark, Delaware 19716, and Department of Chemistry, University of North Texas, Denton, Texas 76203

Received April 5, 1994®

Abstract: Ethylenediamine (en) solutions of K_3E_7 (E = P, As, Sb) react with toluene solutions of $LM(CO)_3$ (M = Cr, W; L = mesitylene; M = Mo; L = cycloheptatriene) in the presence of 3 equiv of 2,2,2-crypt to give $[K(2,2,2\text{-crypt})]_3[E_7M(CO)_3]$ complexes. Nine $[E_7M(CO)_3]^{3-}$ compounds, **2EM** (E = P, As, Sb and M = Cr, Mo, W), have been prepared and characterized by various physical and spectroscopic techniques. The compounds comprise distorted norbornadiene-like η^4-E_7^{3-} groups bound to C_{3v} $M(CO)_3$ centers. The bonding is described as E_7 π-type interactions with the metal center. ^{13}C and ^{31}P NMR studies and ligand exchange reactions show E_7–$M(CO)_3$ dissociation does not occur in the absence of external oxidants. Simulations of the second-order AA′A″A‴MM′X ^{31}P NMR spectra show large $^1J_{P-P}$ coupling constants (478 Hz, av) associated with the "olefinic" P–P groups of the **2PM** compounds. The ν(CO) bands appear at 1845–1708 cm^{-1} in the IR spectra. The electronic spectra show intense charge-transfer bands for the **2EM** compounds with lower energy $\pi_3 \rightarrow \pi_4$ transitions observed for the **2PM** series. The reactivity of these compounds to form $[HE_7M(CO)_3]^{2-}$ and $[(L_2)M'(CO)_3E_7M(CO)_3]^{3-}$ compounds is discussed. Crystal data for $[K(2,2,2\text{-crypt})]_3[P_7Cr(CO)_3]\cdot en$ at 296 K: a = 14.236(5) Å, b = 14.523(4) Å, c = 20.895(7) Å, α = 80.67(3)°, β = 88.93(3)°, γ = 78.39(3)°, Z = 2, and space group $P\bar{1}$. Crystal data for $[K(2,2,2\text{-crypt})]_3[Sb_7Cr(CO)_3]$ at 243 K: a = 50.300(9) Å, b = 13.897(3) Å, c = 28.433(5) Å, β = 108.43(1)°, Z = 8, and space group $C2/c$.

Introduction

The synthesis and properties of transition metal complexes with bare polyphosphorus ligands are areas of current interest. Many of the early polyphosphorus compounds were prepared from P_4 and unsaturated transition metal complexes and contain μ-P_2, cyclo-P_3, and η^2-P_4 ligands to name a few.[1-9] Under more forcing conditions, higher nuclearity polypnictide fragments are formed such as those in $(\eta^5\text{-}C_5H_4Me)_4Fe_6(CO)_{13}P_8$[10] and $[(Cp''Rh)_2(P_5\text{-}P_5)(RhCp'')_2]$.[11] The corresponding chemistry of the heavier polypnictides arsenic, antimony, and bismuth has been less investigated.[1,4,7,8,12-15]

Aside from P_4 and other forms of elemental pnictogens, there is another class of viable polypnictide precursors, namely the group 15 polyanions. This class of soluble Zintl ions has a rich structural chemistry of its own. Many of the polypnictide anions (and their hydrides)[9,16,17] have cyclic hydrocarbon-like structures such as the nortricyclane E_7^{3-} (I) and trishomocubane E_{11}^{3-} (II) compounds. The structural analogies reside in the fact that E

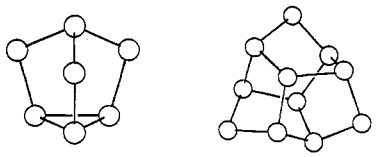

I II

and E^- are electronically equivalent to CH and CH_2, respectively. In a valence bond formalism, one can assign a localized −1 charge to each two-coordinate pnictogen atom.

The reactivities of the group 15 Zintl ions with transition metal complexes have been virtually unexplored with only a few compounds reported to date. The products isolated thus far are quite different from those obtained from elemental precursors under similar reaction conditions. Some of the compounds are prepared in a "rational" manner and are analogous to their hydrocarbon analogues. For example, the $[(\eta^5\text{-}P_5)M(CO)_3]^{1-}$ ions (M = Cr, Mo, W)[18] are prepared from LiP_5 and $M(CO)_6$ precursors and are isostructural to the $[(\eta^5\text{-}C_5H_5)M(CO)_3]^{1-}$ compounds. Similarly, P_7^{3-} reacts with 3 equiv of $(\eta^5\text{-}C_5H_5)Fe(CO)_2Br$ to form $[(\eta^5\text{-}C_5H_5)Fe(CO)_2]_3P_7$[19] in a simple metathesis reaction. Other compounds, such as $^1_\infty[Rb\cdot NbAs_8]^{2-}$ [20] and $[Sb_7Ni_3(CO)_3]^{3-}$,[21] have unprecedented structural types, and their synthetic pathways are not as obvious.

† University of Maryland.
‡ University of Delaware.
§ University of North Texas.
® Abstract published in *Advance ACS Abstracts*, August 15, 1994.

(1) Di Vaira, M.; Sacconi, L. *Angew. Chem., Int. Ed. Engl.* **1982**, *21*, 330–342 and references therein.
(2) von Schnering, H. G.; Hönle, W. *Chem. Rev.* **1988**, *88*, 243–273 and references therein.
(3) Scherer, O. J.; Winter, R.; Wolmershäuser, G. Z. *Anorg. Allg. Chem.* **1993**, *619*, 827–835.
(4) Scherer, O. J. *Angew. Chem., Int. Ed. Engl.* **1985**, *24*, 924–943.
(5) Di Vaira, M.; Stoppioni, P.; Peruzzini, M. *Polyhedron* **1987**, *6*, 351–382 and references therein.
(6) Scherer, O. J. *Comments Inorg. Chem.* **1987**, *6*, 1–22 and references therein.
(7) Scherer, O. J. *Angew. Chem., Int. Ed. Engl.* **1990**, *29*, 1104–1122.
(8) Herrmann, W. A. *Angew. Chem., Int. Ed. Engl.* **1986**, *25*, 56–76 and references therein.
(9) Baudler, M. *Angew. Chem., Int. Ed. Engl.* **1982**, *21*, 492–512.
(10) Barr, M. E.; Adams, B. R.; Weller, R. R.; Dahl, L. F. *J. Am. Chem. Soc.* **1991**, *113*, 3052–3060.
(11) Scherer, O. J.; Höbel, B.; Wolmershäuser, G. *Angew. Chem., Int. Ed. Engl.* **1992**, *31*, 1027–1028.
(12) Di Maio, A. J.; Rheingold, A. L. *Chem. Rev.* **1990**, *90*, 169–190.
(13) Scherer, O. J.; Winter, R.; Heckmann, G.; Wolmershäuser, G. *Angew. Chem., Int. Ed. Engl.* **1991**, *30*, 850–852.
(14) Albright, T. A.; Yee, K. A.; Saillard, J.-Y.; Kahlal, S.; Halet, J. F.; Leigh, J. S.; Whitmire, K. H. *Inorg. Chem.* **1991**, *30*, 1179–1190 and references therein.
(15) von Schnering, H. G. *Angew. Chem., Int. Ed. Engl.* **1981**, *20*, 33–51 and references therein.
(16) Corbett, J. D. *Chem. Rev.* **1985**, *85*, 383–397.
(17) Baudler, M. *Angew. Chem., Int. Ed. Engl.* **1987**, *26*, 419–441.
(18) Baudler, M.; Etzbach, T. *Angew. Chem., Int. Ed. Engl.* **1991**, *30*, 580–582.
(19) Fritz, G.; Hoppe, K. D.; Hönle, W.; Weber, D.; Mujica, C.; Manriquez, V.; von Schnering, H. G. *J. Organomet. Chem.* **1983**, *249*, 63–80.
(20) von Schnering, H. G.; Wolf, J.; Weber, D.; Ramirez, R.; Meyer, T. *Angew. Chem., Int. Ed. Engl.* **1986**, *25*, 353–354.

0002-7863/94/1516-8077$04.50/0

The structure of the former has an As_8^{8-} ring that is reminiscent of S_8 whereas the latter contains a *nido*-Sb_7Ni_3 core that is a new type of 10-atom polyhedron.

We are interested in systematically developing the area of transition metal polypnictide Zintl ion chemistry to determine the structural and chemical diversity of these systems. In particular, we have been investigating the reactions of the E_7^{3-} ions (**1E** where E = P, As, Sb) with various unsaturated transition metal fragments. In this paper, we describe the synthesis, structure, and properties of the $[E_7M(CO)_3]^{3-}$ complexes where E = P, As, Sb and M = Cr, Mo, W. The reactivity of these compounds to form $[HE_7M(CO)_3]^{2-}$ and $[(en)M'(CO)_3P_7M(CO)_3]^{3-}$ complexes is briefly presented and will be described in detail elsewhere.[22] Accounts of the synthesis and structure of $[As_7Cr(CO)_3]^{3-}$ [23] and the structure and bonding of $[Sb_7Mo(CO)_3]^{3-}$ have appeared.[24]

Results and Discussion

Synthesis. Ethylenediamine (en) solutions of K_3E_7 (E = P, As, Sb) react with toluene solutions of $LM(CO)_3$ (M = Cr, W; L = mesitylene; M = Mo; L = cycloheptatriene) in the presence of 3 equiv of 2,2,2-crypt to give $[K(2,2,2\text{-crypt})]_3[E_7M(CO)_3]$ complexes according to eq 1. Nine $[E_7M(CO)_3]^{3-}$ compounds

$$K_3E_7 + LM(CO)_3 + 3(2,2,2\text{-crypt}) \xrightarrow{\text{en/tol}} [K(2,2,2\text{-crypt})]_3[E_7M(CO)_3] + L \quad (1)$$

E = P, As, Sb; M = Cr, Mo, W

L = mesitylene (M = Cr, W), cycloheptatriene (M = Mo)

have been prepared and are generically described by the symbol **2EM** where E denotes the main group element and M denotes the transition metal. The compounds crystallize from solution in reasonable yields (30–80%) with the exceptions of the **2AsMo** and **2SbMo** compounds, which were obtained in low crystalline yields (~3%). ^{31}P NMR spectra of the crude reaction mixtures involving K_3P_7 show virtually quantitative conversions to the **2PM** compounds.

Microanalysis and X-ray analyses of the crystalline solids revealed solvate molecules (en or toluene) for some of the crystalline compounds (see the Experimental Section). The colors of the complexes vary from bright orange for E = P to dark red-orange for E = As and dark red-brown for E = Sb. The W compounds are slightly darker in color than the Mo or Cr complexes. The crystals and their solutions are very air and moisture sensitive. The nine **2EM** compounds have been characterized by elemental analysis, IR, electronic absorption, ^{31}P and ^{13}C NMR spectroscopies, and representative single crystal X-ray diffraction studies. The **2EM** compounds have a distorted (norbornadiene)$Fe(CO)_3$-type structure (III). A qualitative analysis of the electronic structure and bonding was performed with the aid of Fenske–Hall molecular orbital calculations.

As previously noted,[23] eq 1 chemistry and similar reactions involving the synthesis of $[E_9Cr(CO)_3]^{4-}$ ions (E = Sn, Pb)[25,26] do not occur in the absence of 2,2,2-crypt. Structural and NMR

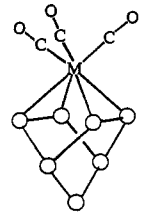

III

spectroscopic studies on K_4Sn_9·HMPA[16,27,28] and ^{31}P NMR spectroscopic studies on Li_3P_7[9,29] clearly reveal significant ion pairing (coordination) between the main group polyanions and the alkali ions in solution and in the solid state. Ion pairing presumably blocks the formation of the $[E_7M(CO)_3]^{3-}$ ions. Upon addition of 3 equiv of 2,2,2-crypt, the ion pairing is diminished and the reaction proceeds slowly at room temperature ($t_{1/2} \approx 3$ h). When less than 3 equiv of 2,2,2-crypt are used in eq 1 chemistry, the reactions do not proceed to completion.

Reactivity. ^{31}P and ^{13}C NMR studies on compounds **2EM** show that E_7–$M(CO)_3$ dissociation does not occur on the NMR time scale at room temperature. Carbonyl–phosphorus coupling is observed for the **2PM** compounds and the three phosphorus environments remain distinct from –60 to 30 °C (see NMR Spectroscopic Studies). Furthermore, in the absence of external oxidants or H^+ sources, compounds **2EM** do not exchange with added E'_7^{3-} ions or $M'(CO)_3$ fragments (E ≠ E', M ≠ M').

The reactions between the **2ECr** compounds and other E'_7^{3-} ions (eq 2) were monitored by ^{13}C NMR spectroscopy and showed no sign of exchange after several days at room temperature or 2 h at 70 °C. In the presence of protio impurities or external oxidants, decomposition is fascile and mixed main-group complexes are formed.[22]

$$\underset{\textbf{2ECr}}{[E_7Cr(CO)_3]^{3-}} + \underset{\textbf{1E'}}{E'^{3-}_7} \not\rightarrow \underset{\textbf{2E'Cr}}{[E'_7Cr(CO)_3]^{3-}} + \underset{\textbf{1E}}{E^{3-}_7} \quad (2)$$

E or E' = P, As, Sb; E ≠ E'

Similar reactions between **2EM** compounds and other $M'(CO)_3$ precursors do not give exchange products **2EM'** and $M(CO)_3$. Instead, bimetallic products are formed of general formula $[(L_2)M'(CO)_3E_7M(CO)_3]^{3-}$, **3EMM'**, where M and M' are Cr, Mo, W; E = P, As, Sb; and L_2 is en, $(DMF)_2$. For example, **2PW** reacts with an additional 1 equiv of (arene)$W(CO)_3$ in en to form $[(en)W(CO)_3P_7W(CO)_3]^{3-}$, **3PWW**, in high yield according to eq 3. The $(en)W(CO)_3$ group is attached to

$$\underset{\textbf{2PW}}{[P_7W(CO)_3]^{3-}} + (\text{arene})W(CO)_3 \xrightarrow{\text{en}} \underset{\textbf{3PWW}}{[(en)W(CO)_3P_7W(CO)_3]^{3-}} + \text{arene} \quad (3)$$

the unique phosphorus atom furthest from the original $W(CO)_3$ fragment (see IV). The synthesis, structure, and properties of compounds **3EMM'** will be described elsewhere.[22]

Compounds **2EM** can also be protonated (eq 4) to form $[HE_7M(CO)_3]^{2-}$ compounds, **4EM**, in good yields. The structures

$$\underset{\textbf{2EM}}{[E_7M(CO)_3]^{3-}} + H^+ \xrightarrow{\text{DMF}} \underset{\textbf{4EM}}{[HE_7M(CO)_3]^{2-}} \quad (4)$$

(21) Charles, S.; Eichhorn, B. W.; Bott, S. G. *J. Am. Chem. Soc.* **1993**, *115*, 5837–5838.
(22) Charles, S.; Eichhorn, B. W.; Fittinger, J. C. Unpublished results.
(23) Eichhorn, B. W.; Haushalter, R. C.; Huffman, J. C. *Angew. Chem., Int. Ed. Engl.* **1989**, *28*, 1032–1033.
(24) (a) Bolle, U.; Tremel, W. *J. Chem. Soc., Chem. Commun.* **1994**, 217–219. (b) Bolle, U.; Tremel, W. *J. Chem. Soc., Chem. Commun.* **1992**, 91–93.
(25) Eichhorn, B. W.; Haushalter, R. C.; Pennington, W. T. *J. Am. Chem. Soc.* **1988**, *110*, 8704–8706.
(26) Eichhorn, B. W.; Haushalter, R. C. *J. Chem. Soc., Chem. Commun.* **1990**, 937–938.
(27) Teller, R. G.; Krause, L. J.; Haushalter, R. C. *Inorg. Chem.* **1983**, *22*, 1809–1812.
(28) Wilson, W. L.; Rudolph, R. W.; Lohr, L. L.; Taylor, R. C.; Pyykko, P. *Inorg. Chem.* **1986**, *25*, 1535–1541.
(29) Baudler, M.; Ternberger, H.; Faber, W.; Hahn, J. *Z. Naturforsch.* **1979**, *34B*, 1690–1697.

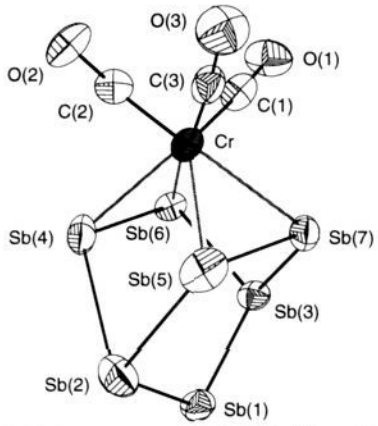

Figure 1. ORTEP drawing of the $[Sb_7Cr(CO)_3]^{3-}$ ion, **2SbCr**, using the common atomic numbering scheme.

of compounds **4EM** are identical to those of **2EM** with the exception of the hydrogen attached to the E atom furthest from the metal atom as illustrated by V. The synthesis, structure, and

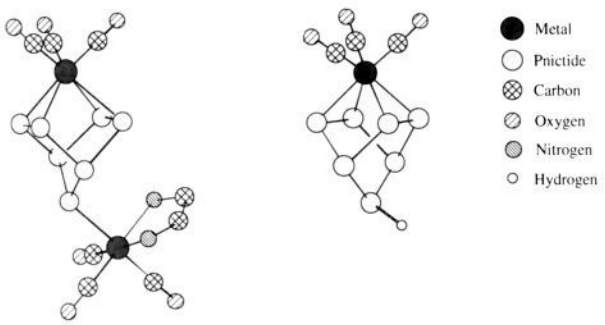

IV V

properties of these compounds will also be described elsewhere;[30] however, the electronic absorption spectra of these compounds are used to aid in the assignment of the electronic transitions of compounds **2EM**.

Solid-State Structures. The compounds **2PCr** and **2SbCr** have been characterized by single crystal X-ray diffraction. The X-ray structures of **2AsCr** and **2SbMo** were reported previously.[23,24] An ORTEP drawing of **2SbCr** is given in Figure 1 as an example of the $[E_7M(CO)_3]^{3-}$ structure type. ORTEP drawings of **2SbCr** and **2PCr** are given in the supplementary material. The crystallographic data are summarized in Table 1 and pertinent bond distances and angles for the three crystallographically characterized Cr compounds are given in Table 2. The fractional coordinates have been deposited in the supplementary material.

The $[E_7M(CO)_3]^{3-}$ structure type contains an η^4-E_7^{3-} group attached to a C_{3v} $M(CO)_3$ center. The ions have C_s molecular symmetry with one mirror plane defined by E(1), M, and C(1). The [K(2,2,2-crypt)]$^+$ salts of the **2PCr** and **2AsCr** ions crystallize in space group $P\bar{1}$, the latter with a toluene solvate[23] and the former with an en molecule hydrogen bonded to the P_7 cage as shown in Figure 2. The two N–P separations average 3.57 Å, which is consistent with hydrogen bonding interactions.[31] The [K(2,2,2-crypt)]$^+$ salts of the $[Sb_7M(CO)_3]^{3-}$ ions where M = Cr, W are isomorphic and crystallize in the monoclinic space group $C2/c$ although molecular C_s symmetry is not crystallographically imposed. The refinement of the $[Sb_7W(CO)_3]^{3-}$ complex was hampered by lack of observed data and will not be reported here.

(30) Charles, S.; Eichhorn, B. W. Unpublished results.
(31) Huheey, J. E.; Keiter, E. A.; Keiter, R. L. *Inorganic Chemistry; Principles of Structure and Reactivity*, 4th ed.; Harper & Row: New York, 1993; p 300.

Table 1. Crytallographic Data for $[K(2,2,2\text{-crypt})]_3[E_7Cr(CO)_3]$ Where E = P, Sb

compound	$[K(2,2,2\text{-crypt})]_3[P_7Cr(CO)_3]\cdot en$	$[K(2,2,2\text{-crypt})]_3[Sb_7Cr(CO)_3]$
formula	$C_{59}H_{116}N_8O_{21}K_3P_7Cr$	$C_{57}H_{108}N_6O_{21}K_3Sb_7Cr$
fw	1659.73	2235.06
space group	$P\bar{1}$	$C2/c$
a, Å	14.236(5)	50.300(9)
b, Å	14.523(4)	13.897(3)
c, Å	20.895(7)	28.433(5)
α, deg	80.67(3)	
β, deg	88.93(3)	108.43(1)
γ, deg	78.39(3)	
V, Å^3	4175.3(26)	18 856(6)
Z	2	8
cryst dimens, mm	0.27 × 0.31 × 0.36	0.36 × 0.40 × 0.46
cryst color	red-orange	dark maroon
D(calcd), g cm^3	1.318	1.574
μ(Mo K$_\alpha$), cm^{-1}	4.72	22.71
temp, K	296	243
2θ scan range, deg	4.0–42.0	4.0–45.0
no. of reflns, colld	9430	13 220
no. of ind. reflns	9284	12 174
no. of ind. obsd reflns $F_o \geq n\sigma(F_o)$	3616 (n = 5)	8158 (n = 4)
$R(F)$, %[a]	10.33	6.75
$R_w(F)$, %[b]	10.45	7.44
Δ/σ(max)	0.019	0.550
GOF	1.74	1.64

[a] $R(F) = \sum||F_o| - |F_c||/\sum|F_o|$. [b] $R_w(F) = (\sum w(|F_o| - |F_c|)^2/\sum wF_o^2)^{1/2}$.

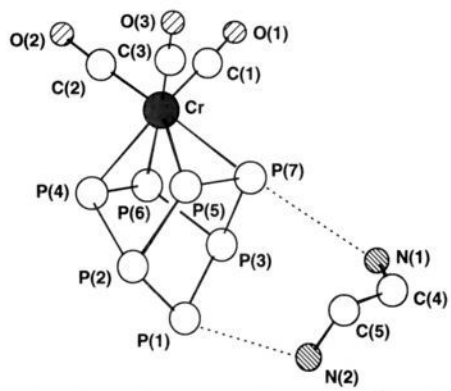

Figure 2. Ball-and-stick drawing of the $[P_7Cr(CO)_3]^{3-}$ ion, **2PCr**, using the common atomic numbering scheme. Dotted lines represent hydrogen bonding interactions.

The Cr–C distances are slightly shorter and the C–O distances slightly longer than those of the neutral $(\eta^6\text{-}C_6H_6)Cr(CO)_3$ precursor [d_{Cr-C} = 1.841 Å, d_{C-O} = 1.158 Å][32] as one would expect from charge considerations and π-back-bonding effects. The virtual C_s symmetry observed in the **2EM** complexes leaves two carbonyl ligands [C(2) and C(3)] in positions *trans* to E(7) and E(6), respectively (average C–M–E angle = 175°). Therefore, there is a slight lengthening of the Cr–E contacts to E(6) and E(7) relative to E(4) and E(5) due to the high *trans* influence of the CO ligands.

It is informative to compare the E–E and M–E contacts for compounds **2EM** to those observed in the $R_2E_2[Cr(CO)_5]_n$ series where E = P, As, Sb and n = 0, 1, 2, 3.[4,33] The n = 0 members are the well-known RE=ER compounds with unbridged E–E double bonds. Schematic drawings of the n = 1 and n = 3 structure types are given in VI and VII. Representative bond distances for these compounds and the **2ECr** ions are listed in Table 3. The E–Cr contacts in the type VI compounds are simple dative bonds with distances quite similar to the E–Cr contacts in $Cr(ER_3)_3$-

(32) Rees, B.; Coppens, P. *Acta Crystallogr.* **1973**, *B29*, 2516–2528.
(33) Cowley, A. H. *Polyhedron* **1984**, *3*, 389–432 and references therein.

Table 2. Selected Bond Distances (Å) and Angles (deg) for the $[E_7Cr(CO)_3]^{3-}$ Ions

	E = P	E = As[a]	E = Sb
	Bonds		
E(1)–E(2)	2.124(10)	2.347(8)	2.721(2)
E(1)–E(3)	2.146(8)	2.370(8)	2.723(2)
E(2)–E(4)	2.237(9)	2.466(8)	2.846(2)
E(2)–E(5)	2.230(8)	2.471(8)	2.845(2)
E(3)–E(6)	2.233(9)	2.453(8)	2.855(2)
E(3)–E(7)	2.212(9)	2.462(8)	2.846(2)
E(4)–E(5)	2.825(8)	3.082(8)	3.331(4)
E(6)–E(7)	3.071(8)	3.292(8)	3.715(4)
E(4)–E(6)	2.128(9)	2.356(9)	2.700(2)
E(5)–E(7)	2.114(8)	2.334(9)	2.707(2)
E(4)–Cr	2.502(6)	2.636(10)	2.804(3)
E(5)–Cr	2.487(6)	2.630(11)	2.807(3)
E(6)–Cr	2.539(7)	2.703(10)	2.848(3)
E(7)–Cr	2.527(6)	2.685(10)	2.850(3)
Cr–C(1)	1.824(7)	1.62(8)	1.877(20)
Cr–C(2)	1.754(20)	1.82(16)	1.812(15)
Cr–C(3)	1.768(21)	1.82(9)	1.827(17)
C(1)–O(1)	1.173(22)	1.15(5)	1.146(24)
C(2)–O(2)	1.224(24)	1.28(5)	1.178(19)
C(3)–O(3)	1.196(26)	1.25(10)	1.176(21)
	Angles		
E(1)–E(2)–E(4)	107.4(4)	107.5(3)	108.1(1)
E(1)–E(3)–E(7)	107.0(3)	105.5(3)	106.2(1)
E(2)–E(1)–E(3)	96.6(3)	97.9(3)	98.5(1)
E(2)–E(4)–E(6)	104.0(3)	104.8(28)	105.9(1)
E(3)–E(7)–E(5)	103.1(3)	104.2(3)	102.9(1)
E(4)–E(2)–E(5)	78.5(3)	77.29(24)	71.7(1)
E(6)–E(3)–E(7)	87.4(3)	84.11(25)	81.3(1)
E(4)–Cr–E(5)	69.0(2)	71.67(27)	72.8(1)
E(4)–Cr–E(6)	49.9(2)	52.36(24)	57.1(1)
E(6)–Cr–E(7)	74.6(2)	75.33(28)	81.4(1)
E(2)–E(4)–Cr	104.4(3)	103.93(27)	104.8(1)
E(3)–C(7)–Cr	99.1(3)	99.64(28)	97.6(1)
E(4)–E(6)–Cr	64.1(2)	62.36(27)	60.6(1)
E(7)–E(5)–Cr	66.0(2)	65.17(28)	62.2(1)
E(4)–Cr–C(1)	140.2(7)	132.7(16)	137.9(5)
E(5)–Cr–C(1)	133.1(6)	140.0(16)	138.8(5)
E(6)–Cr–C(3)	173.3(6)	175.3(17)	176.0(5)
E(7)–Cr–C(2)	172.0(8)	177.9(18)	176.8(5)
Cr–C(1)–O(1)	179.5(15)	170.(4)	175.5(15)
Cr–C(2)–O(2)	174.1(19)	168.(4)	173.5(16)
Cr–C(3)–O(3)	177.3(17)	174.(5)	176.0(15)

[a] Data taken from ref 23.

$(CO)_3$ and related compounds.[34-37] Moreover, the E–E distances (and $^1J_{P-P}$ values) are virtually unchanged from the parent RE=Er-type compounds.[4] In contrast, the E–E distances and the E–Cr contacts to the bridging $Cr(CO)_5$ fragments in type VII compounds are substantially longer than those in type VI. The E–Cr and E–E distances observed for compounds **2ECr** are quite similar to those found for type VII compounds. These similarities are suggestive of a diene-like model in which the E_7^{3-} fragment is attached through π-type interactions. These interactions are discussed in Electronic Structure of $[E_7M(CO_3)]^{3-}$, below.

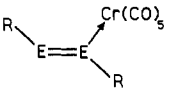

VI

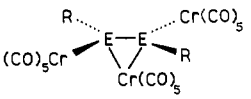

VII

In general, the E–E bonds in the E_7^{3-} fragments of the $[E_7Cr(CO)_3]^{3-}$ ions fall into three categories: four short bonds E(1)–E(2), E(1)–E(3), E(4)–E(6), and E(5)–E(7); four single bond contacts E(3)–E(6), E(3)–E(7), E(2)–E(4), and E(2)–E(5); and a long secondary bond[45] E(4)–E(5). The structural changes that occur in the E_7^{3-} fragment upon complexation are best illustrated by the Sb_7^{3-} [46,47]/$[Sb_7Cr(CO)_3]^{3-}$ pair (Chart 1). The primary distortion occurs by significant lengthening of the Sb(4)–Sb(5) bond of 2.895 Å in Sb_7^{3-} to a secondary bonding distance of 3.331(4) Å in $[Sb_7Cr(CO)_3]^{3-}$. In turn, the nonbonding Sb(6)–Sb(7) contact of 4.296 Å in Sb_7^{3-} is significantly compressed to 3.715 Å in the Cr complex. The changes in bond angles E(4)–E(2)–E(5) [60.0° → 71.7°] and E(6)–E(3)–E(7) [100.5° → 81.3°] also illustrate the E_7 cage distortions upon coordination. The $Cr(CO)_3$ moiety seems to fit the best into the As_7^{3-} fragment in that **2AsCr** displays the smallest overall distortions from the parent E_7^{3-} cluster and shows the least relative E(4)–E(5)/E(6)–E(7) asymmetry of the three structurally characterized Cr compounds. Despite this fact, the E(4)–E(5)/E(6)–E(7) bond asymmetries are quite pronounced for all compounds in the solid state (ΔE–E ≈ 0.20 – 0.35 Å) yet the fluxional nature of the compounds in solution renders the four metal-bound E atoms equivalent on the NMR time scale (see NMR Spectroscopic Studies).

Electronic Structure of $[E_7M(CO)_3]^{3-}$. With the aid of Fenske–Hall molecular orbital (FH MO) calculations,[48-51] we have constructed molecular orbital diagrams for the **2EM** complexes from the constituent C_{3v} $Cr(CO)_3$ and E_7^{3-} fragments with and without E(4)–E(5)/E(6)–E(7) asymmetries. As with any system studied by the FH MO method, one can gain insight into the trends in orbital interactions between compounds but absolute energies and specific orbital orderings are of little value.

The electronic structures of C_{3v} $M(CO)_3$ fragments are well-known.[52] As previously mentioned, the **2EM** structure type is similar to that of (norbornadiene)$Fe(CO)_3$. Accordingly, the metal–ligand interactions in the **2EM** compounds are reminiscent of those in $(\eta^4\text{-}C_4H_4)Fe(CO)_3$ (VIII), with a rectangular distortion

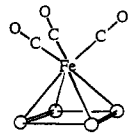

VIII

of the cyclobutadiene ligand.[52] By using this formalism, one obtains an 18-electron configuration at Cr through coordination of a 6-electron E_4^{2-} fragment to the 12-electron $Cr(CO)_3$ center.

(34) Huttner, G.; Schelle, S. *J. Organomet. Chem.* **1973**, *47*, 383–390.
(35) Elmes, P. S.; Gatehouse, B. M.; Lloyd, D. J.; West, B. O. *J. Chem. Soc., Chem. Commun.* **1974**, 953–954.
(36) Plastas, H. J.; Stewart, J. M.; Grim, S. O. *Inorg. Chem.* **1973**, *12*, 265–272.
(37) Wieber, M.; Graf, N. *Z. Anorg. Allg. Chem.* **1993**, *619*, 1991–1997.
(38) Yoshifuji, M.; Shima, I.; Inamoto, N.; Hirotsu, K.; Higuchi, T. *J. Am. Chem. Soc.* **1981**, *103*, 4587–4589.
(39) Cowley, A. H.; Norman, N. C.; Pakulski, M. *J. Chem. Soc., Dalton Trans.* **1985**, 383–386.
(40) Yoshifuji, M.; Hashida, T.; Inamoto, N.; Kirotsu, K.; Horiuchi, T.; Higuchi, T.; Ito, K.; Nagase, S. *Angew. Chem., Int. Ed. Engl.* **1985**, *24*, 211–212.
(41) Cowley, A. H.; Lasch, J. G.; Norman, N. C.; Pakulski, M. *Angew. Chem., Int. Ed. Engl.* **1983**, *22*, 978–979.
(42) Borm, J.; Zsolnai, L.; Huttner, G. *Angew. Chem., Int. Ed. Engl.* **1983**, *22*, 977–978.
(43) Huttner, G.; Schmid, H. G.; Frank, A.; Orama, O. *Angew. Chem., Int. Ed. Engl.* **1976**, *15*, 224.
(44) Weber, U.; Huttner, G.; Scheidsteger, O.; Zsolnai, L. *J. Organomet. Chem.* **1985**, *289*, 357–366.
(45) Alcock, N. W. *Adv. Inorg. Chem. Radiochem.* **1972**, *15*, 1–53.
(46) Adolphson, D. G.; Corbett, J. D.; Merryman, D. J. *J. Am. Chem. Soc.* **1976**, *98*, 7234–7239.
(47) Critchlow, S. C.; Corbett, J. D. *Inorg. Chem.* **1984**, *23*, 770–774.
(48) Bursten, B. E.; Fenske, R. F. *J. Chem. Phys.* **1977**, *67*, 3138–3145.
(49) Bursten, B. E.; Jensen, R. J.; Fenske, R. F. *J. Chem. Phys.* **1978**, *68*, 3320.
(50) Herman, F.; Skillman, S. *Atomic Structure Calculations*; Prentice-Hall: Englewood Cliffs, NJ, 1963.
(51) Hall, M. B.; Fenske, R. F. *Inorg. Chem.* **1972**, *11*, 768–775.
(52) Albright, T. A.; Burdett, J. K.; Whangbo, M.-H. *Orbital Interactions in Chemistry*; John Wiley & Son, Inc.: New York, 1985; pp 218, 387.

Table 3. Comparison of Bond Distances of RE=ER, RE=ER[Cr(CO)$_5$], and RE=ER[Cr(CO)$_5$]$_3$ with E_4–E_6/E_5–E_7 of the **2ECr** Complexes[a]

	E–E (Å)			E–Cr$_b$(Å)			E–Cr$_t$(Å)		
compd	P	As	Sb	P	As	Sb	P	As	Sb
RE=ER′	2.034(2)[b]	2.244(1)[c]							
RE=ER′{Cr(CO)$_5$}	2.039(3)[d]	2.246(1)[e]					2.354(2)	2.454(1)	
RE=ER′{Cr(CO)$_5$}$_3$	2.125(6)[f]	2.371[g]	2.720(3)[h]	2.524(3)	2.64	2.870(4)	2.405(4)	2.53	2.687(3)
				2.546(5)		2.924(5)	2.411(4)		2.700(4)
2ECr[i]	2.121	2.345	2.704	2.514	2.664	2.827			

[a] See VI and VII for schematic drawings of RE=ER[Cr(CO)$_5$] and RE=ER[Cr(CO)$_5$]$_3$ (Cr$_b$ and Cr$_t$ denote bridging and terminal chromium pentacarbonyl fragments, respectively). [b] R = R′ = [2,4,6-(Me$_3$C)$_3$C$_6$H$_2$].[38] [c] R = R′ = [(Me$_3$Si)$_3$C].[39] [d] R = [2,4,6-(Me$_3$C)$_3$C$_6$H$_2$], R′ = [1,3,5-(Me)$_3$C$_6$H$_2$].[40] [e] R = [2,4,6-(Me$_3$C)$_3$C$_6$H$_2$], R′ = [CH(Me$_3$Si)$_2$].[41] [f] R = R′ = [C$_6$H$_5$].[42] [g] R = R′ = [C$_6$H$_5$].[43] [h] R = R′ = Me$_3$C.[44] [i] Bond distances are averaged (this work).

Chart 1

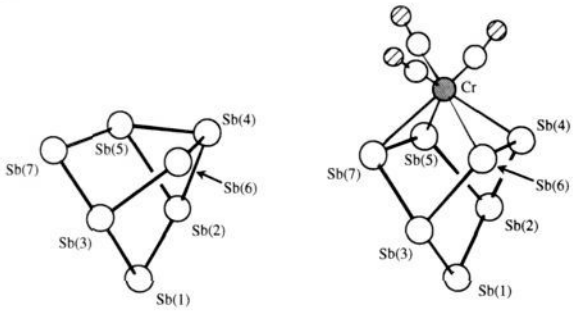

Bond (Å)/Angle (°)	Sb_7^{3-} [a]	$Sb_7Cr(CO)_3^{3-}$
Sb(4)-Sb(5)	2.895	3.331
Sb(6)-Sb(7)	4.296	3.715
Sb(4)-Sb(6)	2.727	2.700
Sb(1)-Sb(3)	2.769	2.723
Cr-C (ave)	---	1.80
C-O (ave)	---	1.18
Sb(6)-Sb(3)-Sb(7)	100.5	81.3
Sb(4)-Sb(2)-Sb(5)	60.0	71.7

[a] Data are averaged.

The other –1 charge of E_7^{3-} is formally localized on the E_7 cage (discussed below).

It is informative to first examine the changes in electronic structure of the E_7^{3-} fragments as one progresses from Sb → As → P. These are shown diagrammatically in Figure 3. In order to illustrate the bonding trends within the E_7^{3-} series, the fragment energies were normalized such that the energies of the π_1 orbitals were equivalent. The P_7^{3-} fragment represents the limiting case of a cyclobutadiene-type system with a rectangular distortion. The two π-bonding orbitals, π_1 ($6a_1$) and π_2 ($4b_2$), fall below the π-antibonding orbitals, π_3 ($5b_1$) and π_4 ($3a_2$), as expected. The lone pair on P(1) is primarily localized in the $5b_2$ fragment orbital with some contribution from the $4b_2$. Due to the relatively strong π interactions between the phosphorus atoms, the π_2 orbital is well below the π_3 orbital. The π bonding diminishes in the E_7^{3-} fragments as one progresses from P → As → Sb as is observed in the RE=ER compounds (E = P, As, Sb).[4,33] Accordingly, the stabilization of π_2 and destabilization of the π_3 decrease such that the two orbitals are virtually degenerate for Sb_7^{3-}. This π_2–π_3 degeneracy represents the undistorted limit for cyclobutadiene[52] due to the lack of p-orbital interaction. For the As_7^{3-} and Sb_7^{3-} fragments, the E(1) lone pairs are almost exclusively associated with the $4b_2$ orbitals and drop below the π_2 orbitals.

The $[E_7Cr(CO)_3]^{3-}$ interaction diagrams were calculated from both atomic basis sets and transformed basis sets of the fragment molecular orbitals in order to trace the origins of the orbital interactions. The molecular orbital diagram for $[As_7Cr(CO)_3]^{3-}$ was the least complicated by mixing and is shown in Figure 4. Again, the energies of the π_1-derived orbitals were normalized to those of **2AsCr** ion in order to illustrate the bonding trends across the series. Because of the low symmetry of the complexes

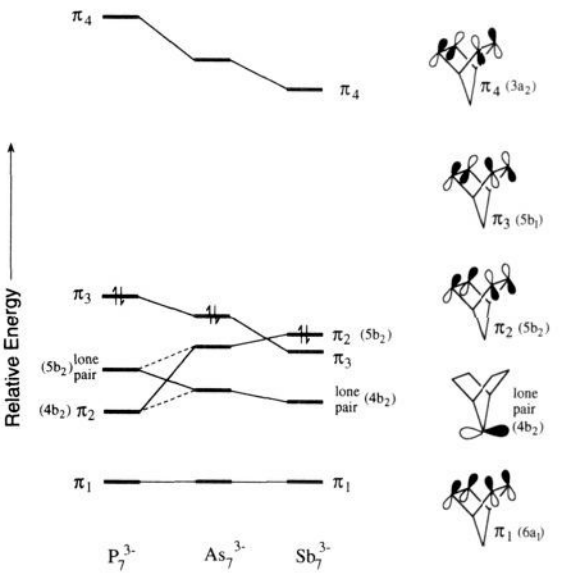

Figure 3. Qualitative molecular orbital diagram for the idealized C_{2v} E_7^{3-} fragments of the $[E_7Cr(CO)_3]^{3-}$ ions where E = P, As, Sb. The energies of the π_1 molecular orbitals were normalized to illustrate the trends in the series.

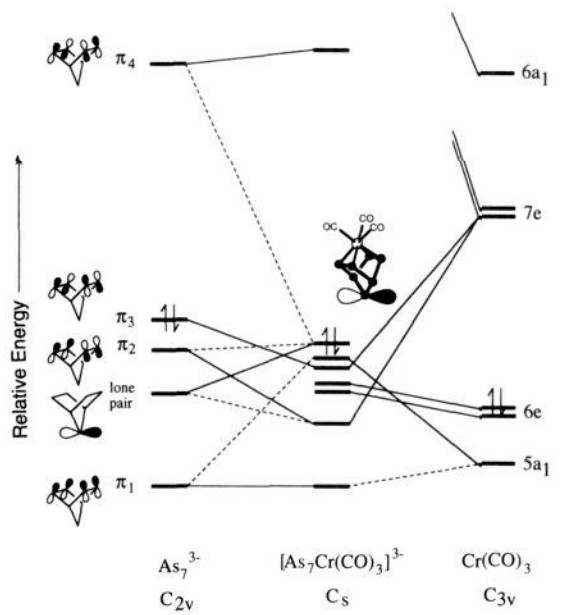

Figure 4. Qualitative molecular orbital diagram for the $[As_7Cr(CO)_3]^{3-}$ complex showing the interactions of the As_7^{3-} and $Cr(CO)_3$ fragments.

(C_s) and the large number of high-lying pnictogen lone pairs, significant orbital mixing was observed in all the E_7^{3-} fragments. However, the major interactions involve the four "π-type orbitals" of the E_7^{3-} fragment in analogy to (η^4-C_4H_4)Fe(CO)$_3$. The

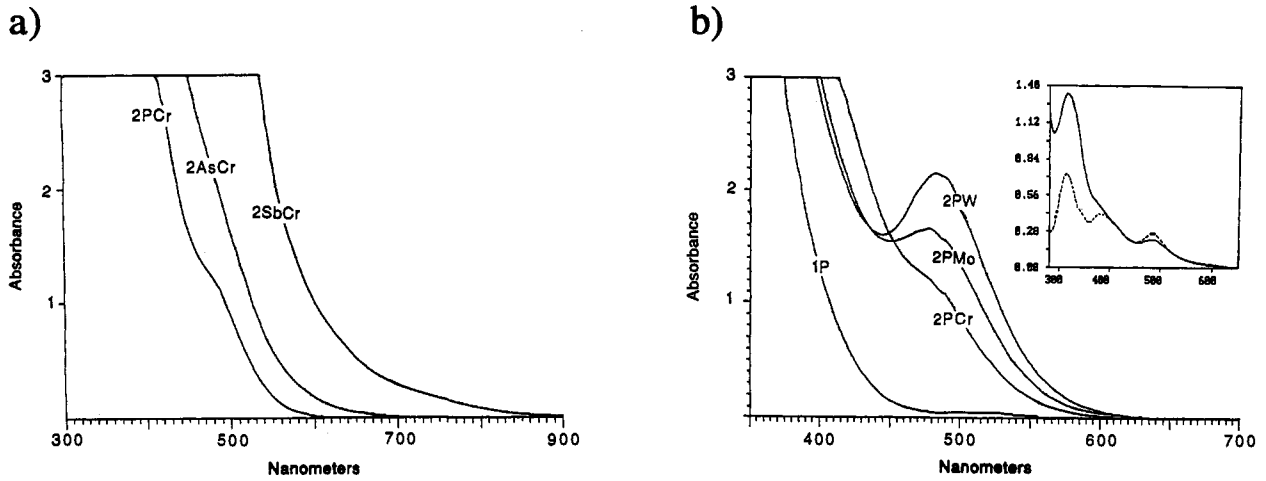

Figure 5. (a) Electronic absorption spectra for the $[E_7Cr(CO)_3]^{3-}$ ions, **2ECr**, where E = P, As, Sb. Spectra were recorded at room temperature from 1.0 mM en solutions. (b) Electronic absorption spectra for the $[P_7M(CO)_3]^{3-}$ ions, **2PM**, where M = Cr, Mo, W. Spectra were recorded at room temperature from 1.0 mM en solutions. The spectrum of P_7^{3-} at the same concentration is given for comparison. The inset shows spectra of $[P_7W(CO)_3]^{3-}$ (solid line) and $[HP_7W(CO)_3]^{2-}$ (dashed line) recorded from 0.1 mM en solutions.

primary orbital interactions involve the stabilization of the π_2 and π_3 E_7^{3-} fragment molecular orbitals upon complexation by interactions with the 7e fragment orbitals of $Cr(CO)_3$. These interactions transfer significant charge onto the $Cr(CO)_3$ fragment, resulting in the destabilization of the filled $5a_1$ and 6e $Cr(CO)_3$ fragment orbitals upon complexation. The charge transfer is evidenced by the changes in Mulliken populations of the respective fragment and molecular orbitals. For example, the π_3 orbitals of the E_7^{3-} fragments are fully occupied with orbital populations of 2.0 electrons but decrease to *ca.* 1.5 electrons for the **2ECr** compounds. Likewise, the initially empty 7e orbitals of the $Cr(CO)_3$ fragments have net populations of *ca.* 1.0 electrons in the complexes. The π_1 and π_4 orbitals essentially come straight across, the latter as the LUMO of all three **2ECr** complexes. It is interesting to note that, in the E_7^{3-} field, the $5a_1$ orbital of the $Cr(CO)_3$ fragment is artificially stabilized[52] relative to the 6e orbital due to the high charge on the complex. Interaction with the E_7^{3-} fragment brings this orbital back up to its "expected" position.[52]

The As(1) lone pair of the As_7^{3-} fragment remains highly localized and comes across as the HOMO of the **2AsCr** ion whereas the lone pair of **2SbCr** is distributed between the HOMO, SHOMO, and a lower lying orbital. In contrast, the lone pair on **2PCr** is localized but is stabilized relative to the other two compounds and is found below the predominantly metal-based HOMO and π_2. This trend can be attributed to the higher electronegativity of P relative to the other pnictogens that allows for increased stabilization of the negative charge associated with the E(1) lone pair (see below). The changes in HOMO orbital type in this series are also consistent with the trends in electronic spectra, as discussed in the next section, but the nature of the lowest energy transitions suggests that the exact orderings of orbitals (and thus the descriptions of the ground states) in Figure 4 are most likely incorrect. The second-order orbital mixing is more pronounced for **2SbCr** relative to the other two, but the general bonding is quite similar.

The Mulliken atomic charges on the E(1) atoms are *ca.* –0.7 and are twice as large as the charges on the η^4-E atoms (*ca.* –0.35). This observation is in accord with the valence bond formalism that leaves a negative charge on two coordinate pnictogens and is consistent with the reactivity of the compounds. For example, electrophiles such as H^+ and $M'(CO)_3$ attack compounds **2EM** at E(1) to form compounds **4EM** (see V and eq 4) and **3EMM'** (see IV and eq 3), respectively.

Finally, the effect of distortion of the E_7^{3-} fragments was examined by monitoring the changes in orbital interactions occurring when the fragment symmetry was lowered from the idealized C_{2v} to the observed ground-state C_s fragment structure with E(4)–E(5)/E(6)–E(7) asymmetries. In all three $[E_7Cr(CO)_3]^{3-}$ analyses, the distorted structures gave lower total energies. The most prominent stabilizations occurred for those orbitals with σ-like character across the shortened E(4)–E(5) contact. Additional mixing occurs upon distortion, and in general, the E(1) lone pair orbitals mix with lower lying orbitals, which also leads to some stabilization. The distortion of the E_7^{3-} cage may be ascribed to a second-order Jahn–Teller effect. The Mulliken atomic charges associated with the four metal-bound E atoms become inequivalent with higher charges associated with E(6) and E(7) (*ca.* –0.4) relative to E(4) and E(5) (*ca.* –0.2). These charges nicely explain the occurrence of hydrogen bonding of the en solvate molecule to the P(7) and P(1) atoms in the crystal structure of $[K(2,2,2\text{-crypt})]_3[P_7Cr(CO)_3]\cdot en$.

In a recent paper by Bolle and Tremel,[24a] the electronic structure of $[Sb_7Mo(CO)_3]^{3-}$, **2SbMo**, was studied by the extended Hückel method. In their analysis, the Sb_7^{3-} fragment of the complex was modeled after the unperturbed Sb_7^{3-} ion with the basal bonds fixed at 2.9 Å. Their analysis showed a similar mechanism of electron transfer from the Sb_7^{3-} fragment to the metal center; however, the analogy to a coordinated diene was not considered. Their viewpoint was based on the decreased elongation of the Sb(4)–Sb(5) bond relative to **2AsCr**. The authors suggested[24a] that this decrease in elongation was due to poorer M–E overlap relative to As–Cr interactions, thus reducing the tendency to "cleave" the E(4)–E(5) bond as effectively as was observed in **2AsCr**. This trend may reflect a relative size effect in which the large Sb_7^{3-} ion does not have to distort (elongate the E(4)–E(5) contact) as much as the smaller E_7^{3-} ions in order to "fit" in the $M(CO)_3$ coordination sphere.

Electronic Spectra. The electronic absorption spectra for the three chromium compounds **2ECr** and the phosphorus compounds **2PM** are shown in Figure 5, parts a and b, respectively. The spectrum of **1P** (with 3 equiv of 2,2,2-crypt) is shown in Figure 5b for comparison. A listing of the λ_{max} values for compounds **2EM** and their molar absorptivities are given in Table 4.

The tails of the intense charge-transfer bands ($\epsilon > 10\,000$ $L\cdot mol^{-1}\cdot cm^{-1}$) in the **2ECr** series (Figure 5a) are red shifted as E changes from P → As → Sb and are relatively insensitive to the nature of the transition metal. Because this behavior is also consistent with the *trend* observed in the **1E** parent clusters, we have assigned these absorbances as intraligand charge-transfer bands. A low-energy shoulder is observed in the **2PCr** spectrum that appears to be buried beneath the charge-transfer bands in the other two spectra. In the **2PM** series (Figure 5b), the lowest energy transition is almost invariant in energy as M changes

Table 4. Spectroscopic Data for **2EM** Complexes

	IR[a]	NMR[b]				UV–vis[c]	
		^{31}P		^{13}C			
compd	ν(C–O) (cm^{-1})	δ (ppm)[d]	J (Hz)[e]	δ (ppm)	J (Hz)[f]	λ_{max}	ϵ (L·cm^{-1}·mol^{-1})
2PCr	1829, 1738, 1716	(A) 199, tp	(D) $^1J_{P-P}$ = 483	246.4	$^2J_{C-P}$ = <2	317	(8 871)
		(B) –21, m	(E) $^1J_{P-P}$ = 370			363	(6 600)
		(C) –143, m	(F) $^1J_{P-P}$ = 238			478	(1 230)
2PMo	1841, 1732, 1721	(A) 168, tp	(D) $^1J_{P-P}$ = 473	238.7	$^2J_{C-P}$ = 3	320	(20 745)
		(B) –16, m	(E) $^1J_{P-P}$ = 370			350	(10 635)
		(C) –157, m	(F) $^1J_{P-P}$ = 241			478	(1 671)
2PW	1837, 1728	(A) 184, tp	(D) $^1J_{P-P}$ = 472	231.7	$^1J_{C-W}$ = 180	319	(18 453)
		(B) –8.5, m	(E) $^1J_{P-P}$ = 369		$^2J_{C-P}$ = 5	370	(5 100)
		(C) –160, m	(F) $^1J_{P-P}$ = 238			486	(2 163)
2AsCr	1824, 1741, 1708			247.1		365	(11 400)
2AsMo	1840, 1744, 1720						
2AsW	1836, 1744, 1714			232.4	$^1J_{C-W}$ = 178		
2SbCr	1823, 1748, 1718			245.1		365	(16 000)
2SbMo	1845, 1759, 1730						
2SbW	1842, 1756, 1726			230.7	$^1J_{C-W}$ = 176		

[a] KBr pellets. [b] ^{31}P NMR (DMF-d_7), ambient temperature, 81.015 MHz; ^{13}C NMR (DMF-d_7), ambient temperature, 100.614 MHz. [c] Solvent was ethylenediamine. [d] t = triplet, p = pentent, m = multiplet. (A) P(1). (B) P(2), P(3). (C) P(4), P(5), P(6), P(7). See Figure 2 for the general atomic numbering scheme. [e] (D) $J_{P_4-P_6}$, $J_{P_5-P_7}$. (E) $J_{P_1-P_2}$, $J_{P_1-P_3}$. (F) $J_{P_2-P_4}$, $J_{P_2-P_5}$, $J_{P_3-P_6}$, $J_{P_3-P_7}$. [f] Coupling constants were determined with negative line broadening. LB = 1 was used for spectra in Figure 8.

from Cr → Mo → W with $\lambda_{max} \approx 480$ nm. Instead, only an increase in molar absorptivity is observed with values of 1230, 1671, and 2163 L·mol^{-1}·cm^{-1}, respectively. It is also informative to compare the spectrum of **2PW** to its protonated analog, **4PW** (see insert of Figure 5b). The 480-nm absorbance does not significantly change upon protonation, indicating that the transition is not n → π^* in character. On the basis of these data, we assign the 480-nm band as the $\pi_3 \rightarrow \pi_4$ transition.

On the basis of the qualitative orbital analysis, one might expect low-energy M → π_4 charge transfer and n → π_4 type transitions in the electronic absorption spectra of the **2ECr** compounds. As mentioned previously, the exact ordering of orbitals shown in Figure 4 is probably incorrect and should only be used as a guide in examining trends. In addition, the n → π_4 transitions should be characteristically weak and may be hidden beneath the tails of the other transitions.

IR Spectroscopic Studies. The IR spectra (KBr pellet) for compounds **2EM** show ν(C–O) stretching vibrations between 1845 and 1708 cm^{-1} (see Table 4). The ν(C–O) region for the **2PM** series is shown in Figure 6. The low ν(C–O) values reflect the high negative formal charge on the ion and significant CO π-back-bonding.

In C_s symmetry, the ν(C–O) modes have 2a′ + a″ symmetry and are IR allowed. In most low-symmetry organometallic compounds containing a C_{3v} M(CO)$_3$ fragment, such as Fe(CO)$_3$-(cyclooctatetraene)[53] with C_s point symmetry, the observed ν-(C–O) modes reflect the local C_{3v} symmetry of the M(CO)$_3$ fragment, showing only two bands (a_1 + e). The true molecular symmetry is not reflected in the C–O vibrations due to the low effective mass of the attendant group relative to the M(CO)$_3$ fragment. In contrast, compounds with C_s symmetry and massive attendant groups on the M(CO)$_3$ fragments (i.e., $Pb_9Cr(CO)_3^{4-}$)[26] show the expected three well-resolved ν(C–O) modes reflecting their true point symmetries. Compounds **2EM** are intermediate between these extremes, showing virtual C_{3v} ν(C–O) patterns for the heaviest M and lightest E combination, **2PW**, with splitting of the e band into its a′ + a″ components for the other E–M combinations.

NMR Spectroscopic Studies. The calculated and observed ^{31}P NMR spectra of **2PCr** are shown in Figure 7 and are representative of the **2PM** series. The ^{31}P NMR data are summarized in Table 4. The spectra show three resonances in a 4:2:1 integral ratio corresponding to the four metal-bound atoms [P(4), P(5), P(6), P(7)], the two bridging atoms [P(2) and P(3)], and the unique phosphorus atom P(1), respectively. On the basis of the solid-state structures, AA′BB′MM′X spin systems would be anticipated. However, the spectra are consistent with AA′A″A‴MM′X spin systems, indicating that the compounds are fluxional on the NMR time scale at room temperature. That is, the asymmetries in the

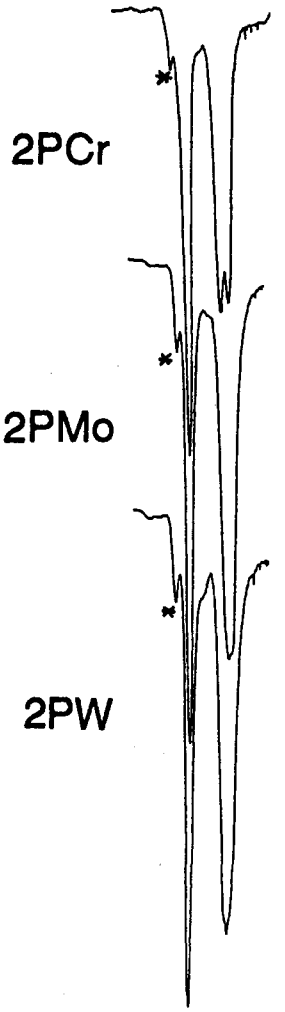

Figure 6. Solid-state IR spectra (KBr pellets) showing the carbonyl regions of the $[P_7M(CO)_3]^{3-}$ complexes, **2PM**, where M = Cr, Mo, W. The high-energy bands marked with the asterisks arise from $[HP_7M(CO)_3]^{2-}$ impurities. See Table 4 for ν(C–O) values.

(53) Deganello, G. *Transition Metal Complexes of Cyclic Polyolefins*; Academic Press: New York, 1979; pp 197–199.

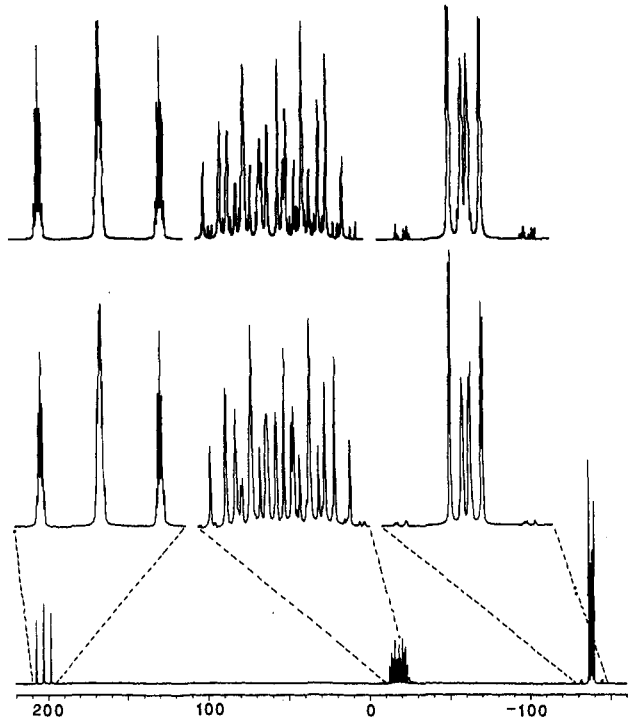

Figure 7. Calculated (top) and observed (middle and bottom) ^{31}P NMR spectra for $[P_7Cr(CO)_3]^{3-}$ recorded at 27 °C and 81.0 MHz from DMF-d_7 solutions. See Table 4 for chemical shifts and coupling constants.

P(4)–P(5)/P(6)–P(7) separations observed in the solid state are time averaged in solution (an intramolecular wagging process), generating virtual C_{2v} symmetries in the P_7 fragments. Exchange remains rapid on the NMR time scale (no signal broadening) at −60 °C in DMF.

The ^{31}P NMR spectra of the **2PM** compounds were simulated in order to extract the P–P coupling constants. The P(4)–P(6) and P(5)–P(7) contacts (2.121 Å, av), which presumably have multiple bond character, are among the shortest observed in the crystal structure of **2PCr**. Although the P(1)–P(2) and P(1)–P(3) contacts are also quite short (2.135 Å, av), the P–P coupling constants are indicative of P–P single bonds. The calculated $^1J_{P-P}$ values for the P(4)–P(6) [or P(5)–P(7)] interactions are 478 Hz (av) for the **2PM** compounds. As expected, these values are less than the $^1J_{P-P}$ coupling constants observed for the RP=PR diphosphene complexes (550–670 Hz)[33] but larger than the coupling constants associated with short P–P single bonds in related polyphosphorus compounds (200–430 Hz).[54,19]

The ^{13}C NMR data for compounds **2EM** are also summarized in Table 4 and representative ^{13}C carbonyl resonances are shown in Figure 8. The chemical shifts range from 230 to 247 ppm with deshielding increasing as **2EW < 2EMo < 2ECr** as the transition metal is varied and **2SbM < 2PM < 2AsM** as the E_7^{3-} group is varied. The influence of the transition metals on the carbonyl chemical shifts parallels those of the $M(CO)_6$ compounds, where M = W (δ = 192.1), Mo (δ = 202.0), and Cr (δ = 212.1),[55] and the related $[HM(CO)_5]^{1-}$ ions.[56] The relative shifts in these series do not correlate with ν(C–O) values and are presumably governed by paramagnetic terms in the chemical shift equation.[55] In general, however, there is a downfield shift of the carbonyl resonances relative to the $M(CO)_6$ and $[HM(CO)_5]^{1-}$ series, where M = Cr, Mo, W, that is consistent with increased carbyne-like character due to M–C multiple bonding.

The carbonyl resonances for the **2EW** and **2PM** compounds show coupling to ^{183}W (I = $^1/_2$, 14% abundance) and ^{31}P, respectively, as shown in Figure 8. The $^1J_{W-C}$ values range from 176 to 180 Hz and increase as **2SbW < 2AsW < 2PW**, which parallels the trends in ν(C–O) values but is opposite to expectations based on electronegativity. The $^2J_{P-C}$ coupling constants for the **2PM** compounds range from 5 to ≤2 Hz according to the series **2PW < 2PMo < 2PCr**.

Conclusions

A series of $[E_7M(CO)_3]^{3-}$ ions (**2EM** where E = P, As, Sb and M = Cr, Mo, W) has been prepared from E_7^{3-} "Zintl" ions and (arene)$M(CO)_3$ precursors. The compounds contain distorted norbornadiene-like E_7^{3-} units bound η^4 to the $M(CO)_3$ fragments. They are fluxional in solution but do not dissociate into the parent $LM(CO)_3$ and E_7^{3-} fragments. The formation of the **2EM** complexes affects structural rearrangements of the E_7^{3-} clusters, generating π-type character (diene-like) between the two pairs of metal-bound pnictogens. The compounds have been studied by NMR, electronic absorption, and IR spectroscopies as well as bonding analyses. The bonding is reminiscent to that in (η^4-C_4H_4)$Fe(CO)_3$, where the frontier $M(CO)_3$ orbitals interact with the diene-like π system. The structural and spectroscopic features of the metal–ligand interactions are quite similar to those of the $E_2R_2[M(CO)_5]_3$ complexes, where the bridging $M(CO)_5$ fragments insert into the E=E double bonds.

The reactivity of compounds **2EM** remains ligand based throughout the series. The lone pair on E(1) is quite nucleophilic and the site of attack by various electrophiles (*e.g.*, H^+, $W(CO)_3$(en), Me_3Si^+, etc.) which will be described elsewhere.[22,30] Preliminary studies on the isoelectronic $[E_7ML]^{3-}$ series of compounds (where M = Pt, L = PPh_3; M = Ni, L = CO, E = P, As) are suggestive of metal-based reactivity that is in sharp contrast to the chemistry of the **2EM** compounds (*e.g.*, the formation $[E_7Pt\mathit{H}(PPh_3)]^{2-}$ versus $[\mathit{H}E_7M(CO)_3]^{2-}$). These transition metal Zintl ion complexes provide an excellent opportunity to systematically study the interactions of main group atoms with transition metals. Further studies are in progress.

Experimental Section

General Data. All reactions were performed in a Vacuum Atmospheres Co. drybox under dinitrogen atmospheres. All IR spectra were recorded from KBr pellets on a Nicolet Model 5DXC FTIR spectrophotometer under dinitrogen purge. Spectral data are listed individually below (s = strong, m = medium, and w = weak). Elemental analyses were performed under inert atmospheres by Schwarzkopf Microanalytical Laboratories, Woodside, NY, and Desert Analytics, Tucson, AZ. Ambient-temperature ^{13}C (100.614 MHz) and ^{31}P (81.015 MHz) NMR spectra were recorded on Bruker AM400 and WP200 spectrometers, respectively. The ^{31}P NMR data were referenced against an external 85% H_3PO_4/CD_2Cl_2 standard (0 ppm). Instruments were run unlocked for samples in ethylenediamine (en) and locked for samples in DMF-d_7. Negative line broadening was used to extract coupling constants from some ^{13}C data. Spectral simulations were performed with the NMR-II simulation software package on a Macintosh computer. Electronic absorption spectra were recorded on a Milton Roy Spectronic 3000 Array spectrophotometer or a Perkin Elmer Lambda 2S spectrometer at ambient temperature using matching, modified anaerobic quartz cells with ethylenediamine as the solvent.

Materials. The K_3E_7 (E = P, As, Sb) reagents were prepared by fusing stoichiometric ratios of the elements in evacuated, sealed silica tubes. *CAUTION*: alkali polyphosphorous compounds are known to spontaneously detonate even under rigorously anaerobic conditions. These materials should only be prepared in small quantities and should be handled with caution. Ethylenediamine solutions of the E_7^{3-} ions were prepared by extracting finely ground powders of the K_3E_7 alloys. The K_3P_7 and K_3As_7 reagents dissolved completely, but the K_3Sb_7 powders were only partially soluble (~80%) under the conditions given below. (Mesitylene)-chromium tricarbonyl, (cycloheptatriene)molybdenum tricarbonyl, (mesitylene)tungsten tricarbonyl, and 4,7,13,16,21,24-hexaoxa-1,10-diazabicyclo-[8.8.8]hexacosane (2,2,2-crypt) were purchased from Aldrich and used without further purification. Ethylenediamine (en) was purchased from

(54) Ali, A. A. M.; Bocelli, G.; Harris, R. K.; Fild, M. *J. Chem. Soc., Dalton Trans.* **1980**, 638–644.
(55) Braterman, P. S.; Milne, D. W.; Randall, E. W.; Rosenberg, E. *J. Chem. Soc., Dalton Trans.* **1973**, 1027–1031.
(56) Darensbourg, M. Y.; Slater, S. *J. Am. Chem. Soc.* **1981**, *103*, 5914–5915.

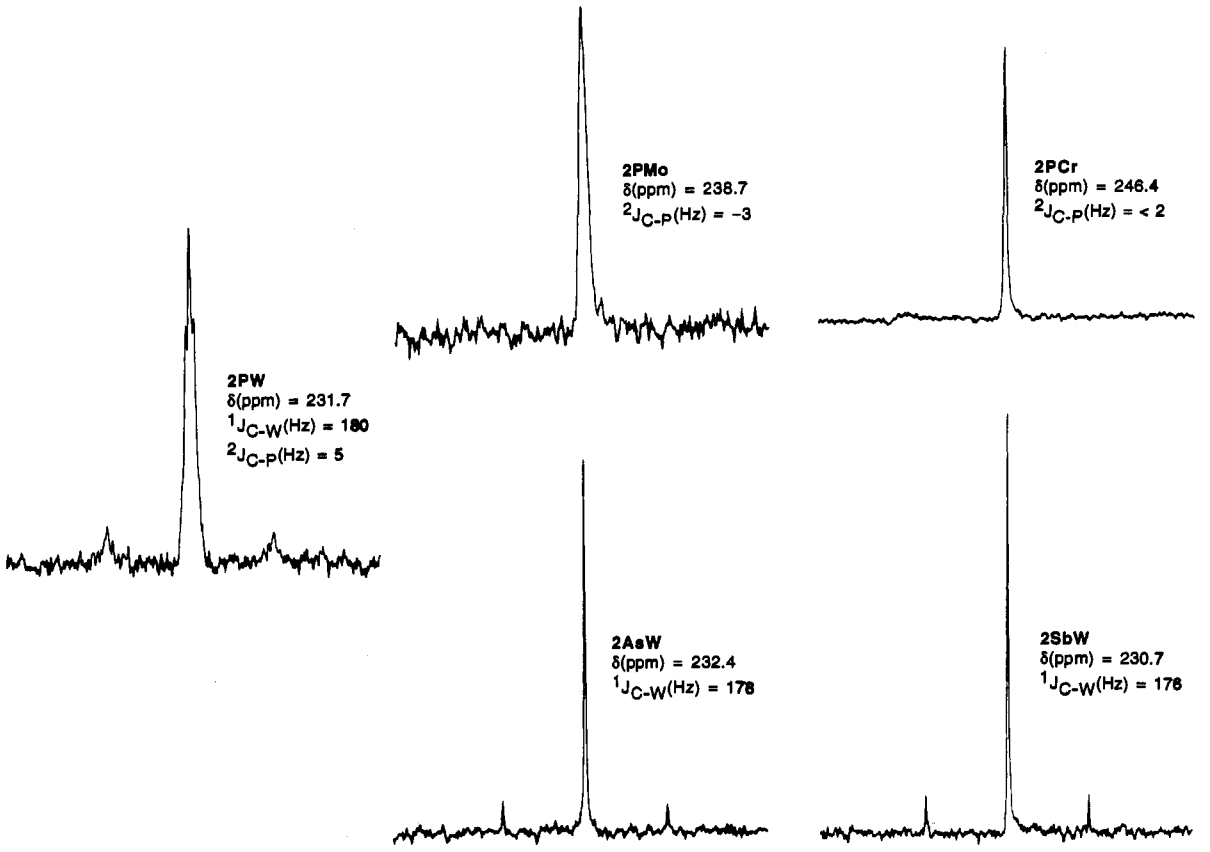

Figure 8. ^{13}C NMR spectra showing the carbonyl resonances of representative $[E_7M(CO)_3]^{3-}$ complexes, **2EM**, where E = P, As, Sb and M = Cr, Mo, W. Spectra were recorded at 27 °C and 100.6 MHz from DMF-d_7 solutions.

Fisher (Anhydrous), distilled from CaH_2 under dinitrogen, then from K_4Sn_9 under dinitrogen, and finally stored under dinitrogen over molecular sieves. Toluene was distilled from sodium/benzophenone under dinitrogen and stored under dinitrogen over molecular sieves. DMF-d_7 was purchased from Cambridge Isotope Laboratories.

Syntheses. [K(2,2,2-crypt)]$_3$[P$_7$Cr(CO)$_3$]-en. In vial 1, K_3P_7 (29.6 mg, 0.089 mmol) and 2,2,2-crypt (100 mg, 0.27 mmol) were dissolved in en (~3 mL), producing a yellow-orange solution. In vial 2, $[C_6H_3(CH_3)_3]Cr(CO)_3$ (22.7 mg, 0.089 mmol) was dissolved in toluene (~1 mL), producing a yellow solution. The contents of vial 2 were added dropwise to the contents of vial 1, yielding a red solution. The reaction mixture was stirred for 4 h, concentrated *in vacuo* to 2 mL, and filtered through *ca.* $^1/_4$ in. of tightly packed glass wool in a pipet. After 24 h, the reaction vessel contained rectangular red-orange crystals that were removed from the mother liquor, washed with toluene, and dried *in vacuo* (crystalline yield, 109 mg, 74%). IR (KBr pellet), cm^{-1}: 2960 (m), 2879 (m), 2813 (m), 1829 (s), 1738 (s), 1716 (s), 1659 (w), 1478 (m), 1459 (m), 1438 (m), 1403 (m), 1387 (s), 1360 (s), 1352 (s), 1296 (m), 1261 (m), 1231 (w), 1173 (w), 1129 (s), 1099 (s), 1082 (s), 1055 (m), 1027 (w), 947 (m), 932 (m), 829 (m), 806 (m), 750 (w), 669 (m), 629 (w). Anal. Calcd for $C_{59}H_{116}N_8O_{21}K_3P_7Cr$: C, 42.70; H, 7.04; N, 6.75; P, 13.06. Found: C, 42.35; H, 6.51; N, 5.21; P, 12.08. Two additional microanalyses did not produce better values.

[K(2,2,2-crypt)]$_3$[As$_7$Cr(CO)$_3$]-tol. A procedure identical to that described earlier for [Rb(2,2,2-crypt)]$_3$[As$_7$Cr(CO)$_3$]-tol was followed except K_3As_7 (56.8 mg, 0.089 mmol) was used in the reaction instead of Rb_3As_7.[23] After 24 h, the reaction vessel contained rectangular dark red crystals. The crystals were removed from the mother liquor, washed with toluene, and dried *in vacuo* (crystalline yield, 54 mg, 31%). IR (KBr pellet), cm^{-1}: 2966 (m), 2879 (m), 2813 (m), 1824 (s), 1741 (s), 1708 (s), 1657 (w), 1479 (m), 1459 (m), 1444 (m), 1401 (m), 1389 (s), 1361 (s), 1352 (s), 1299 (m), 1261 (m), 1238 (w), 1173 (w), 1130 (s), 1102 (s), 1083 (s), 1061 (m), 1029 (w), 948 (s), 931 (m), 830 (m), 818 (m), 754 (w), 667 (m).

[K(2,2,2-crypt)]$_3$[Sb$_7$Cr(CO)$_3$]. A procedure identical to that described for [K(2,2,2-crypt)]$_3$[P$_7$Cr(CO)$_3$]-en above was followed except K_3Sb_7 (85.8 mg, 0.089 mmol) was used in the reaction. After 24 h, the reaction vessel contained rectangular dark red crystals. The crystals were removed from the mother liquor, washed with toluene, and dried *in vacuo* (crystalline yield, 77 mg, 38%). IR (KBr pellet), cm^{-1}: 2954 (m), 2882 (m), 2815 (m), 1823 (s), 1748 (s), 1718 (s), 1599 (w), 1474 (m), 1459 (m), 1440 (m), 1404 (m), 1386 (s), 1360 (s), 1352 (s), 1297 (m), 1258 (m), 1237 (w), 1172 (w), 1131 (s), 1099 (s), 1082 (s), 1058 (m), 1027 (w), 947 (s), 930 (m), 828 (m), 817 (m), 750 (w), 663 (m). Anal. Calcd for $C_{57}H_{108}N_6O_{21}K_3Sb_7Cr$: C, 30.63; H, 4.87; N, 3.76; Sb, 38.13; Cr, 2.33. Found: C, 31.44; H, 5.24; N, 5.33; Sb, 36.66; Cr, 2.12.

[K(2,2,2-crypt)]$_3$[P$_7$Mo(CO)$_3$]-en. In vial 1, K_3P_7 (29.6 mg, 0.089 mmol) and 2,2,2-crypt (100 mg, 0.27 mmol) were dissolved in en (~3 mL), producing a yellow-orange solution. In vial 2, $(C_7H_8)Mo(CO)_3$ (24.1 mg, 0.089 mmol) was dissolved in toluene (~2 mL) and gently heated to give a red solution. Not all of the molybdenum complex dissolved into the toluene. The contents of vial 2, including the undissolved molybdenum complex, were added dropwise to the contents of vial 1, producing a red solution. The reaction mixture was stirred for 4 h, during which time the remaining $(C_7H_8)Mo(CO)_3$ dissolved. The volume was concentrated *in vacuo* to 1 mL and filtered through *ca.* $^1/_4$ in. of tightly packed glass wool in a pipet. After 12 h, the reaction vessel contained small red crystals. The crystals were removed from the mother liquor, washed with toluene, and dried *in vacuo* (crystalline yield, 67 mg, 44%). IR (KBr pellet), cm^{-1}: 2962 (m), 2878 (m), 2818 (m), 1876 (w), 1841 (s), 1732 (s), 1721 (s), 1654 (m), 1476 (m), 1460 (m), 1443 (m), 1398 (m), 1385 (s), 1360 (s), 1352 (s), 1297 (m), 1260 (m), 1237 (w), 1172 (w), 1130 (s), 1101 (s), 1083 (s), 1061 (m), 1029 (w), 948 (s), 930 (m), 829 (m), 820 (m), 751 (w), 661 (m), 618 (w). Anal. Calcd for $C_{59}H_{116}N_8O_{21}K_3P_7Mo$: C, 41.60; H, 6.86; N, 6.58; P, 12.73. Found: C, 42.05; H, 6.99; N, 6.99; P, 12.47.

[K(2,2,2-crypt)]$_3$[As$_7$Mo(CO)$_3$]. A procedure identical to that described for [K(2,2,2-crypt)]$_3$[P$_7$Mo(CO)$_3$]-en was followed except K_3As_7 (56.8 mg, 0.089 mmol) was used in the reaction. After 24 h, the reaction vessel contained a few very small red crystals. The crystals were removed from the mother liquor, washed with toluene, and dried *in vacuo* (crystalline yield, *ca.* 5 mg, 3%). Yields were not optimized. The remaining species in solution are unknown at present. IR (KBr pellet), cm^{-1}: 2955 (m), 2883 (m), 2815 (m), 1891 (w), 1866 (w), 1840 (s), 1744 (s), 1720 (s), 1651 (w), 1475 (m), 1458 (m), 1444 (m), 1401 (m), 1385 (s), 1360 (s), 1354 (s), 1299 (m), 1259 (m), 1238 (w), 1173 (w), 1130 (s), 1102 (s), 1083 (s), 1056 (m), 1031 (w), 948 (s), 933 (m), 829 (m), 820 (m), 753 (w), 698 (w), 617 (w).

[K(2,2,2-crypt)]$_3$[Sb$_7$Mo(CO)$_3$]. A procedure identical to that described for [K(2,2,2-crypt)]$_3$[P$_7$Mo(CO)$_3$]·en was followed except K_3Sb_7 (85.8 mg, 0.089 mmol) was used in the reaction. After 24 h, the reaction vessel contained a few very small red crystals. The crystals were removed from the mother liquor, washed with toluene, and dried *in vacuo* (crystalline yield, *ca.* 7 mg, 3%). Yields were not optimized. The remaining species in solution are unknown at present. IR (KBr pellet), cm^{-1}: 2958 (m), 2879 (m), 2804 (m), 1845 (s), 1759 (s), 1730 (s), 1656 (w), 1483 (m), 1464 (m), 1446 (m), 1400 (m), 1385 (s), 1363 (s), 1356 (s), 1302 (m), 1260 (m), 1238 (w), 1172 (w), 1136 (s), 1100 (s), 1076 (s), 1063 (m), 1025 (w), 941 (s), 933 (m), 830 (m), 819 (m), 751 (w), 614 (w).

[K(2,2,2-crypt)]$_3$[P$_7$W(CO)$_3$]·en. In vial 1, K_3P_7 (29.6 mg, 0.089 mmol) and 2,2,2-crypt (100 mg, 0.27 mmol) were dissolved in en (~3 mL), producing a yellow-orange solution. In vial 2, [C$_6$H$_3$(CH$_3$)$_3$]W(CO)$_3$ (34.4 mg, 0.089 mmol) was dissolved in toluene (~1 mL), producing an orange solution. The contents of vial 2 were added dropwise to the contents of vial 1, yielding a red solution. The reaction mixture was stirred for 2 h, concentrated *in vacuo* to 1.5 mL, and filtered through *ca.* 1/4 in. of tightly packed glass wool in a pipet. After 3 h, the reaction vessel contained rectangular red crystals. The crystals were removed from the mother liquor, washed with toluene, and dried *in vacuo* (crystalline yield, 140 mg, 88%). IR (KBr pellet), cm^{-1}: 2961 (m), 2885 (m), 2813 (m), 1879 (w), 1839 (s), 1729 (s), 1594 (w), 1474 (m), 1458 (m), 1444 (m), 1401 (w), 1384 (s), 1360 (s), 1354 (s), 1299 (m), 1259 (m), 1238 (w), 1171 (w), 1130 (s), 1099 (s), 1083 (s), 1057 (m), 1028 (w), 949 (s), 932 (m), 829 (m), 818 (m), 753 (w). Anal. Calcd for $C_{59}H_{116}N_8O_{21}K_3P_7W$: C, 39.55; H, 6.53; N, 6.25. Found: C, 39.53; H, 6.79; N, 6.50.

[K(2,2,2-crypt)]$_3$[As$_7$W(CO)$_3$]·en. A procedure identical to that described for [K(2,2,2-crypt)]$_3$[P$_7$W(CO)$_3$]·en was followed except K_3As_7 (56.8 mg, 0.089 mmol) was used in the reaction. After 12 h, the reaction vessel contained rectangular red crystals. The crystals were removed from the mother liquor, washed with toluene, and dried *in vacuo* (crystalline yield, 54 mg, 31%). IR (KBr pellet), cm^{-1}: 2955 (m), 2881 (m), 2812 (m), 1888 (w), 1836 (s), 1744 (s), 1713 (s), 1597 (w), 1475 (m), 1456 (m), 1445 (m), 1402 (w), 1386 (s), 1360 (s), 1352 (s), 1297 (m), 1258 (m), 1239 (w), 1174 (w), 1130 (s), 1101 (s), 1084 (s), 1056 (m), 1030 (w), 948 (s), 932 (m), 830 (m), 812 (m), 753 (w). Anal. Calcd for $C_{59}H_{116}N_8O_{21}K_3As_7W$: C, 33.76; H, 5.57; N, 5.34. Found: C, 33.53; H, 5.59; N, 5.61.

[K(2,2,2-crypt)]$_3$[Sb$_7$W(CO)$_3$]. A procedure identical to that described for [K(2,2,2-crypt)]$_3$[P$_7$W(CO)$_3$]·en was followed except K_3Sb_7 (85.8 mg, 0.089 mmol) was used in the reaction. The reaction mixture was stirred for 2 h, concentrated *in vacuo* to 2 mL, and filtered through *ca.* 1/4 in. of tightly packed glass wool in a pipet. During filtration rectangular dark red crystals began to form in the reaction vessel. The crystals were removed from the mother liquor, washed with toluene, and dried *in vacuo* (crystalline yield, 61 mg, 29%). IR (KBr pellet), cm^{-1}: 2958 (m), 2882 (m), 2811 (m), 1842 (s), 1760 (s), 1728 (s), 1602 (w), 1472 (m), 1458 (m), 1444 (m), 1402 (w), 1385 (s), 1361 (s), 1352 (s), 1297 (m), 1259 (m), 1238 (w), 1171 (w), 1131 (s), 1101 (s), 1083 (s), 1056 (m), 1027 (w), 949 (s), 932 (m), 831 (w), 807 (m). Anal. Calcd for $C_{57}H_{108}N_6O_{21}K_3Sb_7W$: C, 28.93; H, 4.60; N, 3.55. Found: C, 27.89; H, 4.81; N, 3.97.

Preparation of UV/Vis Samples. In a drybox, crystalline [K(2,2,2-crypt)]$^+$ salts of **2ECr** and **2PM** ions were dissolved in en in 10-mL volumetric flasks to produce 2.5 mM stock solutions. Stepwise dilutions were then performed to obtain 1.0 mM and 0.1 mM sample solutions which were stored in a drybox. For analysis, an aliquot of each dilute solution was placed in a quartz cell which was stoppered with a rubber septum.

Preparation of Ligand Exchange Samples. The crystalline [K(2,2,2-crypt)]$^+$ salts of **2ECr** (E = P, As, Sb) ions were dissolved in DMF-d_7 (~1/2 mL). Separately, 1 equiv of $K_3E'_7$ (E ≠ E' = P, As, Sb) and 3 equiv of 2,2,2-crypt were dissolved in en (~1/2 mL) and allowed to react for at least 24 h. The $E'_7{}^{3-}$ solution was then combined with the **2ECr** solution. Reactions were monitored by ^{13}C NMR spectroscopy over 7-day periods.

X-ray Crystallography for [K(2,2,2-crypt)]$_3$[Sb$_7$Cr(CO)$_3$] and [K(2,2,2-crypt)]$_3$[P$_7$Cr(CO)$_3$]·en. Crystals suitable for X-ray structural determination were mounted in glass capillaries under dinitrogen gas. Crystal data collection and refinement parameters for both complexes are collected in Table 1. The unit-cell parameters were obtained from the least-squares fit of 25 reflections ($10° \le 2\theta \le 20°$). Photographic evidence and cell reduction routines indicated $\bar{1}$ Laue symmetry for [K(2,2,2-crypt)]$_3$[P$_7$Cr(CO)$_3$]·en. The chemically sensible results of refinement established the space group as $P\bar{1}$. A semiempirical absorption correction factor for absorption was applied to the data set.[57] The systematic absences in the diffraction data for [K(2,2,2-crypt)]$_3$[Sb$_7$Cr(CO)$_3$] established the space group as *Cc* or *C*2/*c*. The *E*-statistics suggested the centrosymmetric alternative, and the chemically sensible results of refinement established the space group as *C*2/*c*. A semiempirical absorption correction factor was applied to the data set (216 Ψ-scans, T_{max}/T_{min} = 1.168).

The structures were solved by direct methods which located the Cr, K, Sb, and P atoms. The remaining non-hydrogen atoms were located through subsequent difference Fourier syntheses. No hydrogen atoms were added to the structures. All atoms were refined with anisotropic thermal parameters except for the carbon atoms in [K(2,2,2-crypt)]$_3$[P$_7$Cr(CO)$_3$]·en. Because of the large lattice size and poor scattering associated with the [K(2,2,2-crypt)]$^+$ ions, complexes of this type are often plagued by high final residuals.[20,23,24,47] The final difference maps were essentially featureless. All software and the sources of the scattering factors are contained in the SHELXTL PLUS (4.2) program library.[58]

Computational Procedures. Molecular orbital calculations were performed by using the Fenske–Hall method that has been described elsewhere.[48-51] SCF calculations were performed in the atomic basis on the E_7^{3-} fragments, the C_{3v}-Cr(CO)$_3$ fragment, and the [E$_7$Cr(CO)$_3$]$^{3-}$ complexes. To aid in the analysis of the orbital interactions, the converged wave functions were transformed into the appropriate transformed bases. The internuclear distances were obtained from crystal data and averaged where appropriate. A common Cr(CO)$_3$ fragment with d_{C-O} = 1.20 Å and d_{Cr-C} = 1.76 Å was used for all structural models. Calculations were performed on idealized symmetrical complexes as well as the observed unsymmetrical structures. The symmetrical models containing C_{2v}-E_7^{3-} fragments were constructed by averaging the crystallographically determined Cr–E contacts and E(4)–E(5)/E(6)–E(7) distances and corresponding angles. The interatomic distances and angles for the unsymmetrical models were taken directly from the crystallographic data. All calculations were performed on a Macintosh IIcx personal computer using the Fenske–Hall program, version 5.1.[51]

The basis functions (single ζ) were generated by the numerical Xα atomic orbital program of Herman and Skillman[50] used in conjunction with the Xα-to-Slater basis program of Bursten and Fenske.[48,49] The Cr atoms were assumed to have cationic $d^{n+1}s^0$ configurations whereas the ground-state atomic configurations were used for the remainder of the atoms. A complete listing of exponents and coefficients used in the basis functions are given in the supplementary material.

Acknowledgment. B.W.E. acknowledges the General Research Board and the Department of Chemistry at the University of Maryland for support of this work. S.G.B. acknowledges the Robert A. Welch foundation for partial support of this work.

Supplementary Material Available: Text describing X-ray crystallography, complete listings of positional parameters, thermal parameters, and bond distances and angles, ORTEP drawings of the **2SbCr** and **2PCr**·en complexes, and a listing of exponents and coefficients used in the FH MO basis functions (32 pages); structure factor tables (55 pages). This materials is contained in many libraries on microfiche, immediately follows this article in the microfilm version of the journal, and can be ordered from the ACS; see any current masthead page for ordering information.

(57) *Crystallographic Computing*; Ahm, F. R., Ed.; Munksgaard: Copenhagen, 1970.
(58) Sheldrick, G. Siemens XRD, Madison, WI.